



SACRED HEART RESEARCH PUBLICATIONS

Journal of Functional Materials and Biomolecules

Journal homepage: www.shcpub.edu.in



ISSN: 2456-9429

Synthesis and characterization of Polypyrrole-Copper ferrite nanocomposites

K.S. Vadivoo¹, S.Krishnan^{2*}, D. Pathinettam Padiyan³

Received on 21 Dec 2016, Accepted on 1 Mar 2017

ABSTRACT

Polypyrrole is prepared by chemical oxidation method using ammonium persulphate $[(\text{NH}_4)_2\text{S}_2\text{O}_8]$ as oxidant. Copper ferrite is prepared by co-precipitation method. Polypyrrole-copper ferrite nanocomposite is prepared by in situ polymerization of pyrrole in aqueous solution with three different concentrations such as 75% pyrrole & 25% copper ferrite (CS I), 50% pyrrole & 50% copper ferrite (CS II) and 25% pyrrole & 75% copper ferrite (CS III). The prepared samples are characterized by XRD, UV-Vis spectroscopy, FT-IR, SEM and A.C. impedance spectroscopy methods. SEM studies reveal that the polypyrrole has a quasi-spherical structure. The grain sizes of the samples are found out using Debye-Scherrer formula. The strain in the prepared samples is found out using Williamson-Hall plot. Fourier Transform Infra Red spectroscopy studies results confirm the formation of polypyrrole and copper ferrite. Ultra violet spectroscopy studies show that the optical band gap of the material changes on addition of copper ferrite.

Keywords: X-ray diffraction; Optical studies; SEM analysis.

1 Introduction

Organic-Inorganic composites with an organized structure usually provide a new functional hybrid with synergetic or complementary behavior between organic and inorganic materials, which have attracted considerable attention for their potential applications [1, 2]. The desire to create structures that combine the mechanical flexibility, optical properties and electrical properties of conducting polymers with the high electrical conductivity and magnetic properties of metals has inspired the development of several techniques for the controlled growth of composites of metals and polymers. In recent years there has been a tremendous increase in materials that are both magnetic and electrically conductive, which have potential applications such as electromagnetic shielding (EMS), molecular electronics, nonlinear optics, microwave absorption and catalysis [3, 4]. Among those multifunctionalized micro/nanostructures, electromagnetic functionalized micro/nanostructures of conducting polymers are of special interest due to their

potential applications in EMS and microwave absorbing materials. Several groups have reported the electromagnetic functional micro/nanostructures of polymer related materials [5, 6]. Polypyrrole (PPY) has provided the possibility of being a good microwave absorbent because of its controllable dielectric loss ability, ease of preparation, good environmental stability and the embedding of nanoparticle (NP) cores inside the conducting PPY is of interest because of the strong electronic interaction between the NPs and the polymer matrices [7, 8]. Magnetic composites materials comprise a new generation of multifunctional materials that combine the properties of ordinary polymer and magnetic materials that one could call magnetopolymeric materials [9].

2 Experimental

2.1 Preparation of Polypyrrole (PPy):

Polypyrrole is prepared by chemical oxidation method. 0.06 M of pyrrole monomer is added with 0.12 M of ammonium persulphate $[(\text{NH}_4)_2\text{S}_2\text{O}_8]$ with constant stirring at about 10°C for about 2 hours to get polypyrrole.

2.2 Preparation of Copper ferrite:

Copper ferrite is prepared by Co-precipitation method. 0.5 M of $\text{Cu}(\text{NO}_3)_2 \cdot 3\text{H}_2\text{O}$ and 1 M of $\text{Fe}(\text{NO}_3)_3 \cdot 9\text{H}_2\text{O}$ are dissolved in 250 ml of distilled water and heated to 90°C with constant stirring for about 2 hours. Then this soln is added with 188 ml of 8 M NaOH which is heated at 90°C for 2 hours, with constant stirring. Then the whole reaction mixture is then heated to 90°C for 2 hours with constant stirring to get a brown precipitate. The pH of the obtained precipitate is reduced to 7, using repeated washing and filtering process. Then the precipitate obtained is dried at 80°C overnight. The powder obtained is sintered at 700°C for about 2 hours to get pure copper ferrite.

2.3 Preparation of Polypyrrole-Copper ferrite nanocomposites:

Polypyrrole-copper ferrite nanocomposites are

* Corresponding author: e-mail: skrishnanjp@gmail.com

¹ Department of Physics, SMK Fomra Institute of Technology, Chennai – 603103, India.

² Department of Physics, B.S.Abdur Rahman University, Vandalur, Chennai – 600048, India.

³ Department of Physics, Manonmaniam Sundaranar University, Tirunelveli-627012, India.

prepared by in-situ chemical oxidative polymerization of pyrrole in the presence of copper ferrite powder, with ammonium persulphate as oxidant. A typical preparation process for polypyrrole-copper ferrite nanocomposites is as follows:-

0.06 M of pyrrole monomer is kept in ultrasonication to obtain a uniform suspension for 30 min. Then copper ferrite powder is added, under ultrasonication for another 30 min. Then ammonium persulphate is added drop by drop for oxidative polymerization under constant stirring, with the temperature maintained at 10°C. Then the powder obtained is filtered, washed with water and dried at 80°C for about overnight. Three samples were prepared, such that the obtained samples contain 75% of polypyrrole and 25% of copper ferrite (CS I), 50% of polypyrrole and 50% of copper ferrite (CS II) and finally 25% polypyrrole and 75% copper ferrite (CS III). These ratios are obtained by changing the mass of copper ferrite powder to be added. The masses of copper ferrite added are 0.0671 gm, 0.279 gm and 0.691 gm to obtain these ratios.

2.4 Characterization:

The morphologies of the samples prepared were characterized by scanning electron microscopy (SEM). The characteristics of the crystallite structure of the prepared samples were determined using an X-Ray diffractometer with CuK_α radiation source. The Fourier transform infrared spectroscopy (FT-IR) of the samples were measured on JASCO FT-IR spectrophotometer with KBr pellets. The ultra violet spectroscopy was measured using TECHCOMP Uv-spectrophotometer. The electrical conductivity of the samples prepared were measured using Lock-In-Amplifier.

3 Results and Discussion

Preparation of polypyrrole from a conventional chemical oxidative polymerization of pyrrole without any surfactants yielded polypyrrole quasi-sphere as reported [10,11] and have an average diameter of about 0.4 μm , with some agglomeration as shown in (fig 1.1). The SEM micrograph of copper ferrite reveals the glassy and hard nature of the material (fig 1.2). The particle size is very fine and found to be less than 0.1 μm . From the micrograph of CS I (fig 1.3), the average particle diameter is found to be 0.33 μm . From the micrograph of CS II (fig 1.4), the average particle diameter is found to be 0.20 μm . From the SEM micrograph of CS III (fig 1.5), the average particle diameter is found to be 0.25 μm . By polymerization of pyrrole monomers in the presence of copper ferrite, it is interestingly found that the produced composites possess sphere like structure and no structure corresponding to copper ferrite powder was distinguished, which indicates that the copper ferrite are uniformly coated with polypyrrole and thus core-shell structure formed is confirmed [12]. It can be seen that the individual

copper ferrite are well coated during the chemical oxidative polymerization of pyrrole. With the increase in the copper ferrite content in polypyrrole-copper ferrite composites, a slight change in diameters of the spherical structures is observed, which is due to the increasing thickness of the copper ferrite cores.

Fig 2 shows the X-ray diffraction (XRD) pattern for the prepared samples. In the XRD pattern of polypyrrole, a broad peak appears at 24.13° which is attributed to the amorphous state of polypyrrole. This peak corresponds to the scattering from bare polymer chains at the inter planar spacing of protonated polypyrrole. The diffraction pattern reveals that the prepared sample is purely amorphous. Fig 2.2 shows the XRD pattern for copper ferrite. It displays a sharp peak at 35.57° which is the characteristic peak of ferrites corresponding to (3 1 1) reflection. The other peaks at 30.35° , 43.62° , 53.47° and 62.59° are observed due to reflections from (2 2 0), (4 0 0), (4 2 2) and (4 4 0) planes respectively. The experimentally measured 'd' values are compared with the standard values (JCPDS No.77-0010) for copper ferrite and good agreement is noticed. The cell parameter and cell volume are calculated using the "UNIT CELL" software and they are found to be 8.343(9) Å and 580 Å³ respectively matches very well with the standard data. Fig2.3 shows the XRD pattern for the sample CS I. The broad peak of polypyrrole around 25° and the characteristic peak of copper ferrite at 35.46° corresponding to spinel ferrite (3 1 1) reflection are found to appear. The diffraction intensity of copper ferrite peak here is less when compared to pure copper ferrite peak. It has been reported that the structure of polypyrrole doped with counter ions are essentially amorphous. The characteristic peaks of polypyrrole and copper ferrite both are found at 24.80° and 35.46° respectively. As the amount of copper ferrite is increased, the intensity of the copper ferrite peak increases which can be seen in the X-ray diffraction patterns of CS II and CS III as shown in Figs 2.4 and 2.5 respectively. With the increase in the content of Copper ferrite in polypyrrole-copper ferrite nanocomposites, the diffraction peak of polypyrrole becomes weaker, while the diffraction peak corresponding to copper ferrite becomes more distinguishable and stronger. For the sample CS III (25% of pyrrole & 75% of copper ferrite), only the diffraction peak referring to copper ferrite can be recognized while the polypyrrole broad peak appears as a hump which may be due to the presence of core-shell structure. Thus XRD analysis also indicates that there is no obvious chemical interaction between copper ferrite and polypyrrole in the nanocomposites but that copper ferrite only serves as the nucleation sites for the polymerization of pyrrole. The formation of core-shell structure is thus confirmed by the XRD analysis. For each sample the grain size for the prominent peaks is calculated using Scherrer's formula ($t = (K\lambda) / (\beta \cos\theta_B)$) and is shown in Table 1.

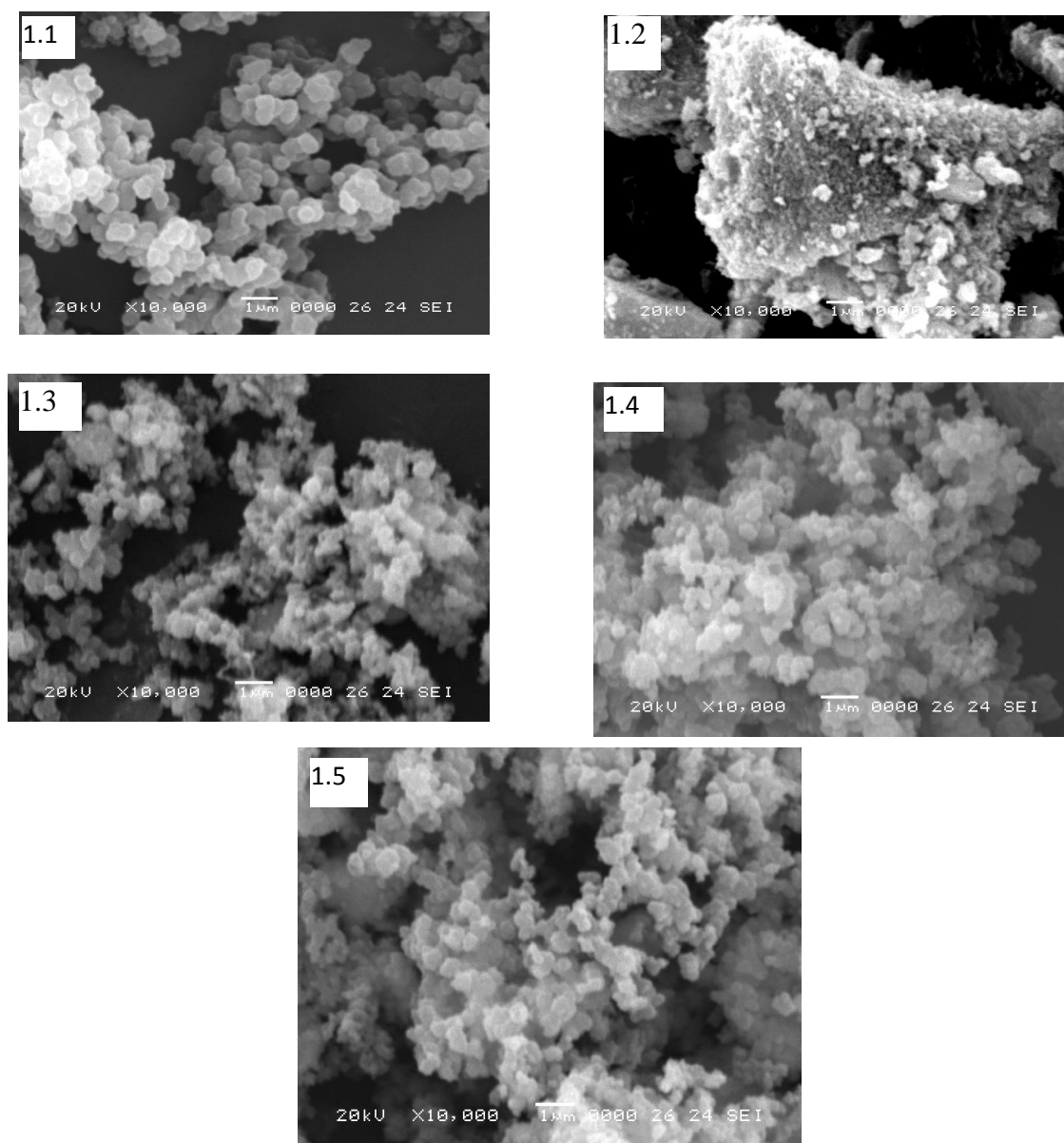


Fig 1. SEM image of PPy (1.1), CuFe₂O₄ (1.2), CS I (1.3), CS II (1.4) and CS III (1.5)

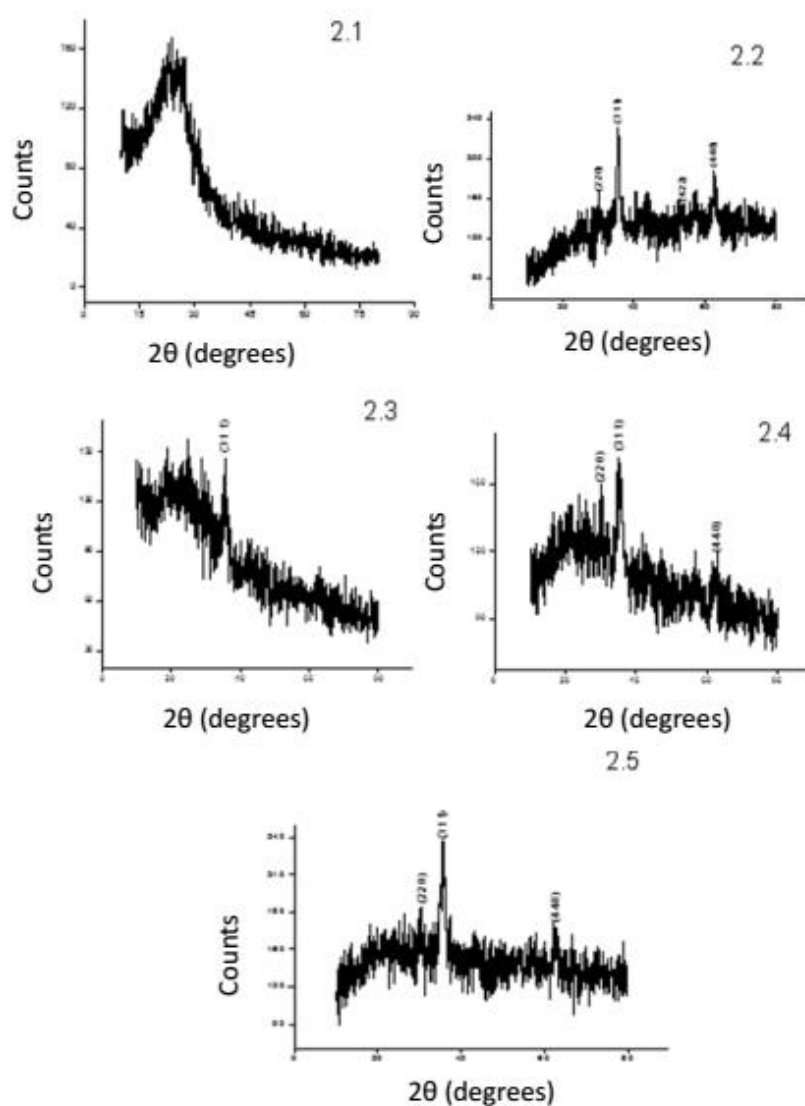


Fig 2. XRD patterns of PPy (2.1), CuFe_2O_4 (2.2), CS I (2.3), CS II (2.4) and CS III (2.5)

Table 1 Grain size of the prepared samples

Sample	Observed 2θ (degrees)	hkl	FWHM (radians)	Grain Size (nm)
Polypyrrole	24.13	-	0.07	1.99
Copper ferrite	35.57	3 1 1	0.03	5.15
	62.59	4 4 0	0.04	3.95
CS I	24.80	-	0.07	1.99
	35.46	3 1 1	0.03	4.54
CS II	35.44	3 1 1	0.03	4.06
	62.27	4 4 0	0.05	2.89
CS III	35.55	3 1 1	0.03	5.22
	62.57	4 4 0	0.07	1.99

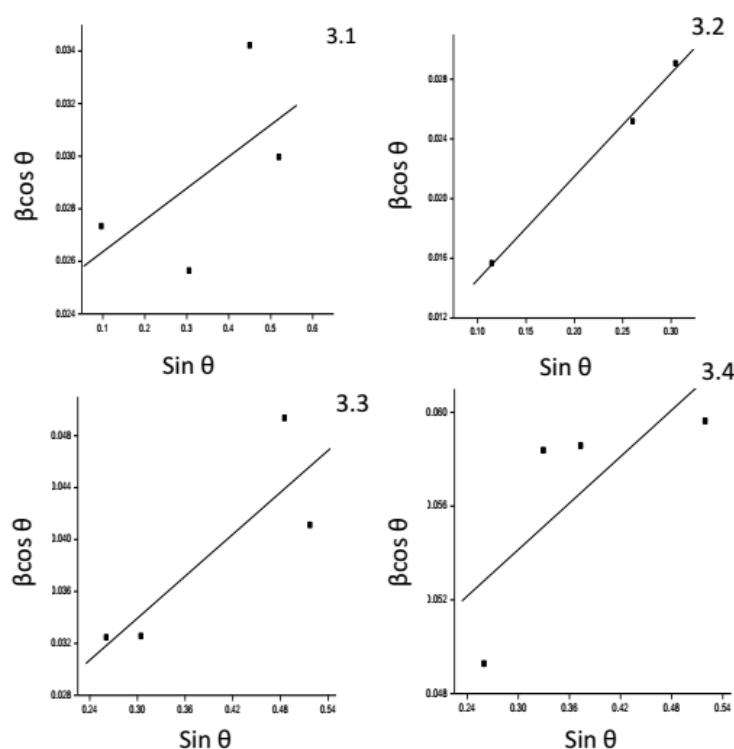


Fig 3. Williamson Hall Plot of CuFe_2O_4 (3.1), CS I (3.2), CS II (3.3), CS III (3.4)

Table 2 Strain in the samples by Williamson Hall method

Sample	Grain Size 't' (nm)	Strain
Copper ferrite	11.43	0.0257
CS I	2.023	0.0129
CS II	2.551	0.0298
CS III	4.271	0.0516

The microstrains present in the prepared samples are found out using Williamson Hall plot as discussed above. The graph between $\beta \cos \theta$ and $\sin \theta$ is drawn. The strain in the sample is calculated using the y intercept and the grain size is calculated from the slope value. The graph between $\beta \cos \theta$ and $\sin \theta$ for the prepared samples are shown in Fig. 3.

FTIR spectra of the prepared samples are displayed in the Fig 4. The bands at 1568 cm^{-1} and 1471 cm^{-1} relate to the fundamental vibrations of the pyrrole

rings. Absorption band around 3439 cm^{-1} could be due to the N-H stretching of polypyrrole. The band from 1214 to 1108 cm^{-1} with a maximum at 1170 cm^{-1} corresponds to C-N stretching vibrations. The band observed at 1042 cm^{-1} corresponds to the N-H in plane deformation vibrations. The FTIR spectrum of copper ferrite prepared by coprecipitation method shows a band at 569 cm^{-1} confirms the presence of ferrite. The bands at 3439 cm^{-1} and 1623 cm^{-1} represent the traces of water present in the sample. In the FTIR spectrum of CS I, the characteristic peaks of pyrrole rings are found in 1568 cm^{-1} and 1471 cm^{-1} . Most of the bands that appeared in polypyrrole appear here also. The characteristic peak of ferrite at 569 cm^{-1} is absent here. This shows that the thickness of shell is more than the core. The FTIR spectrum of CS II also contains most of the bands that appeared in the polypyrrole sample. In addition we can see the characteristic peak of ferrite at 569 cm^{-1} . The FTIR spectrum of CS III also has most of the peaks that are observed in the polypyrrole sample. The ferrite peak is observed with high intensity here when compared to the sample other samples.

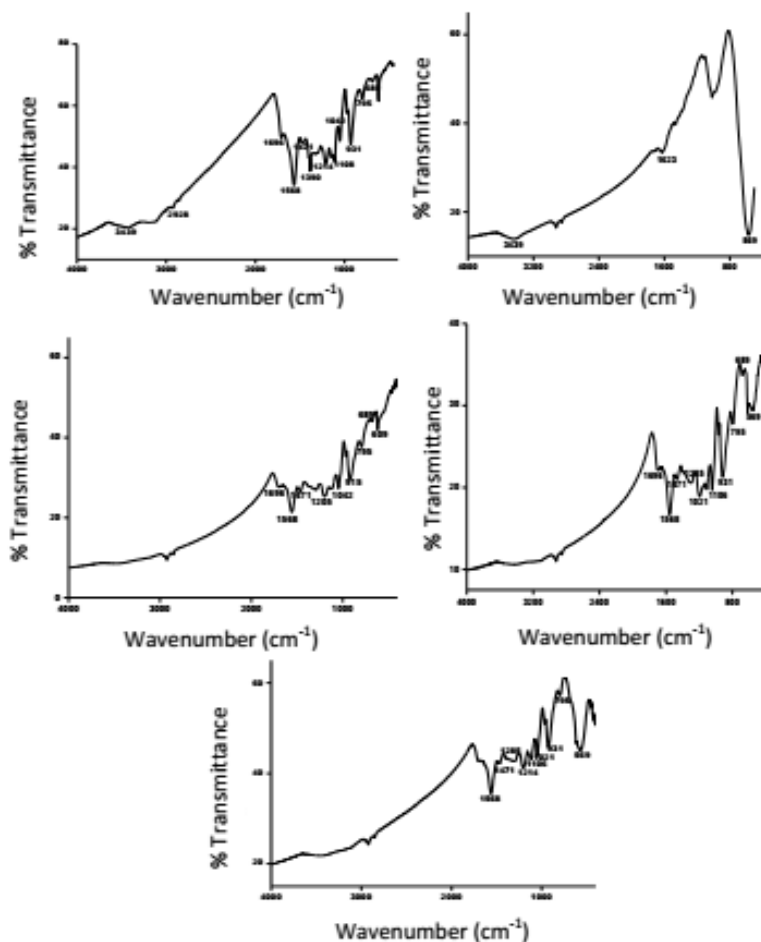


Fig 4. FTIR spectrum of PPy (4.1), CuFe₂O₄ (4.2), CS I (4.3), CS II (4.4), CS III (4.5)

Table 3 Optical band gap of prepared samples

Sample	Band gap (eV)
Polypyrrole	4.30
Copper ferrite	3.76
CS I	4.32
CS II	4.08
CS III	4.19

UV-Vis spectrum is recorded in the wavelength region 200-1100 nm, using UV-Vis spectrophotometer model 2100 manufactured by Techcomp. The sample is prepared by dissolving about 0.004 g of the substance in one drop of H₂SO₄ to which 20ml of water is added. The reference solution contains 1 drop of H₂SO₄ in 20 ml of water. The % absorbance of the samples has been analyzed. From the absorbance spectrum, the optical band gap of the samples has been found using tauc plot using the relation,

$$\alpha h\nu = A (h\nu - E_g)^{1/2}$$

Fig 5 shows the UV-Vis absorption spectrum of all the prepared samples. The absorption spectrum of polypyrrole prepared by chemical oxidation method shows a peak at 298 nm which shows the presence of $\pi \rightarrow \pi^*$ transition, the characteristic transition of aromatic rings, conventional double or triple bonds and carbonyl or azo groups. The UV-Vis absorption spectrum of copper ferrite prepared by co-precipitation method has a peak around 306 nm. The UV-Vis absorption spectrum of the sample CS I has a peak around 298 nm which is the characteristic peak of polypyrrole. The UV-Vis absorption spectrum of the sample CS II has a broad peak around 327 nm. The UV-Vis absorption spectrum of the sample CS III has a broad peak around 321 nm.

Fig 6 shows the plot of $h\nu$ vs. $(\alpha h\nu)^2$ for all the five samples from which the optical band gap of the samples are found. From the tauc plot, the optical band gap of polypyrrole is found to be 4.3 eV. The optical band gap of copper ferrite is found to be 3.76 eV. The optical band gap of CS I is found to be 4.32 eV. From the tauc plot the optical band gap of CS II found to be 4.08 eV. From the tauc plot the optical band gap of CS III is found to be 4.19 eV.

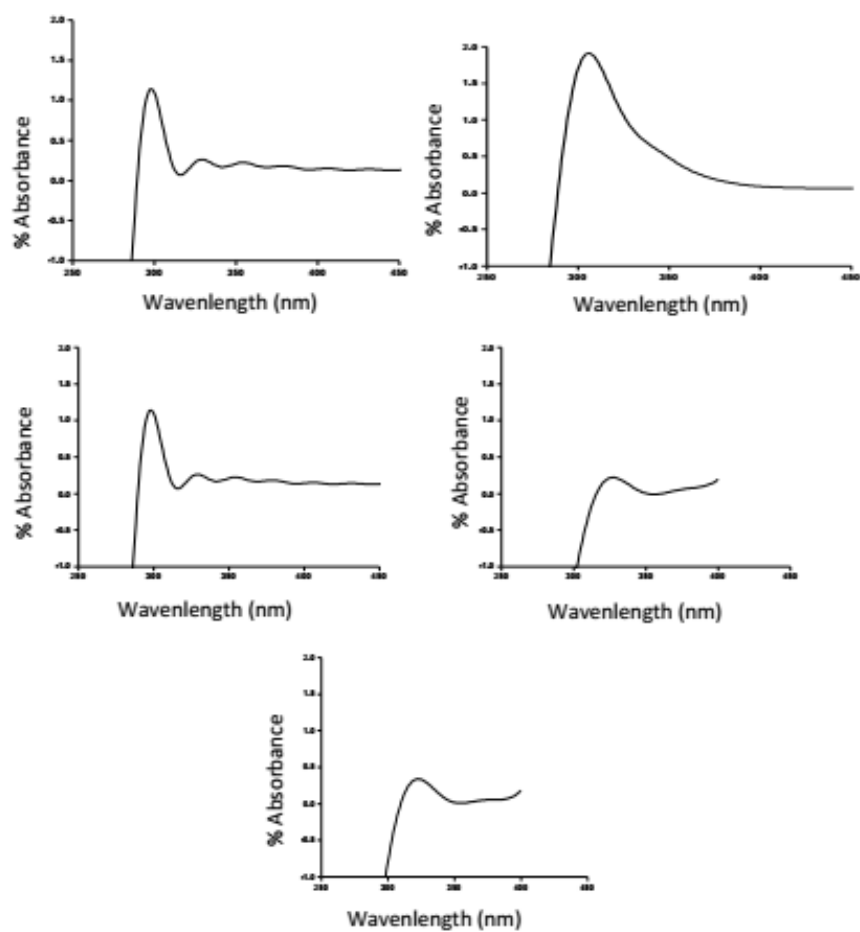


Fig 5. Uv-Vis spectrum of PPy (5.1), CuFe₂O₄ (5.2), CS I (5.3), CS II (5.4), CS III (5.5)

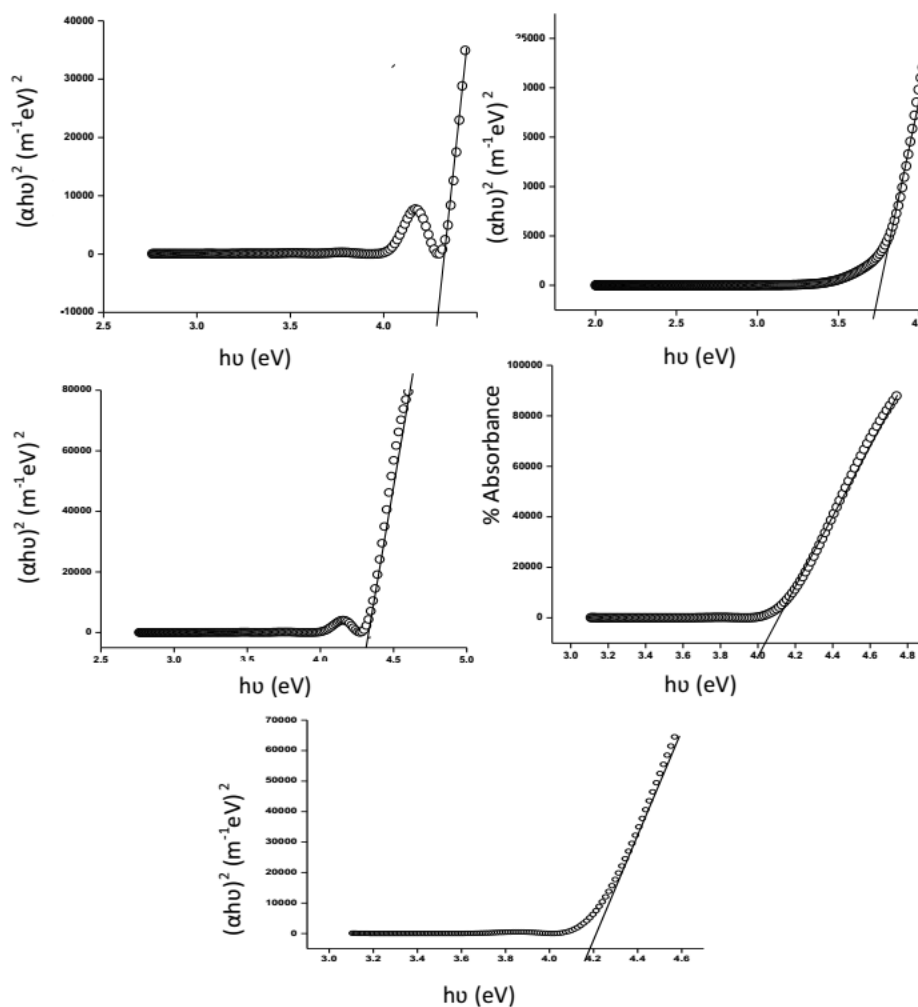


Fig 6. Tauc plot of PPy (6.1), CuFe_2O_4 (6.2), CS I (6.3), CS II (6.4), CS III (6.5)

The a.c. conductivity measurements are carried out using phase sensitive detector Model SR 830 DSP Lock in amplifier. The pelletized samples are placed between the copper electrodes. The input excitation AC signal amplitude is fixed at 0.05V. The frequency is varied from 1 Hz to 100 KHz. The voltage and the phase changes are measured by varying the frequency. The same procedure is repeated by varying the temperature from 303 K to 423 K. From the obtained values the conductivity measurement of the material is carried out. The impedance spectra of polypyrrole at various temperatures are shown in Fig 7.1. The material contains different types of dipoles, each of which has a relaxation time different from others. So the Nyquist Diagram, is not exactly semicircular, but are distorted. The impedance spectra of polypyrrole at various temperatures. The material contain different types of dipoles, each of which has a relaxation time different from others. So the Nyquist Diagram, is not

exactly semicircular, but is distorted. As the temperature increases, the peak tends to broaden indicating the multiple relaxations in the material. The observation of single arc indicates that the circuit components of grain are much higher than that those of a grain boundary and the maximum of the arc in the impedance plot shifts towards low frequency and lies outside the available frequency range as the temperature increases. An equivalent circuit consisting of one parallel combination of resistance and capacitance is usually used to interpret the complex impedance data. The impedance parameters are found out using the Nyquist diagram and tabulated (Table 4.1). From the table it is found that the capacitance and conductivity values increase with increase in temperature, which shows that the sample has a semiconducting behaviour. This is due to the decrease in the resistance value.

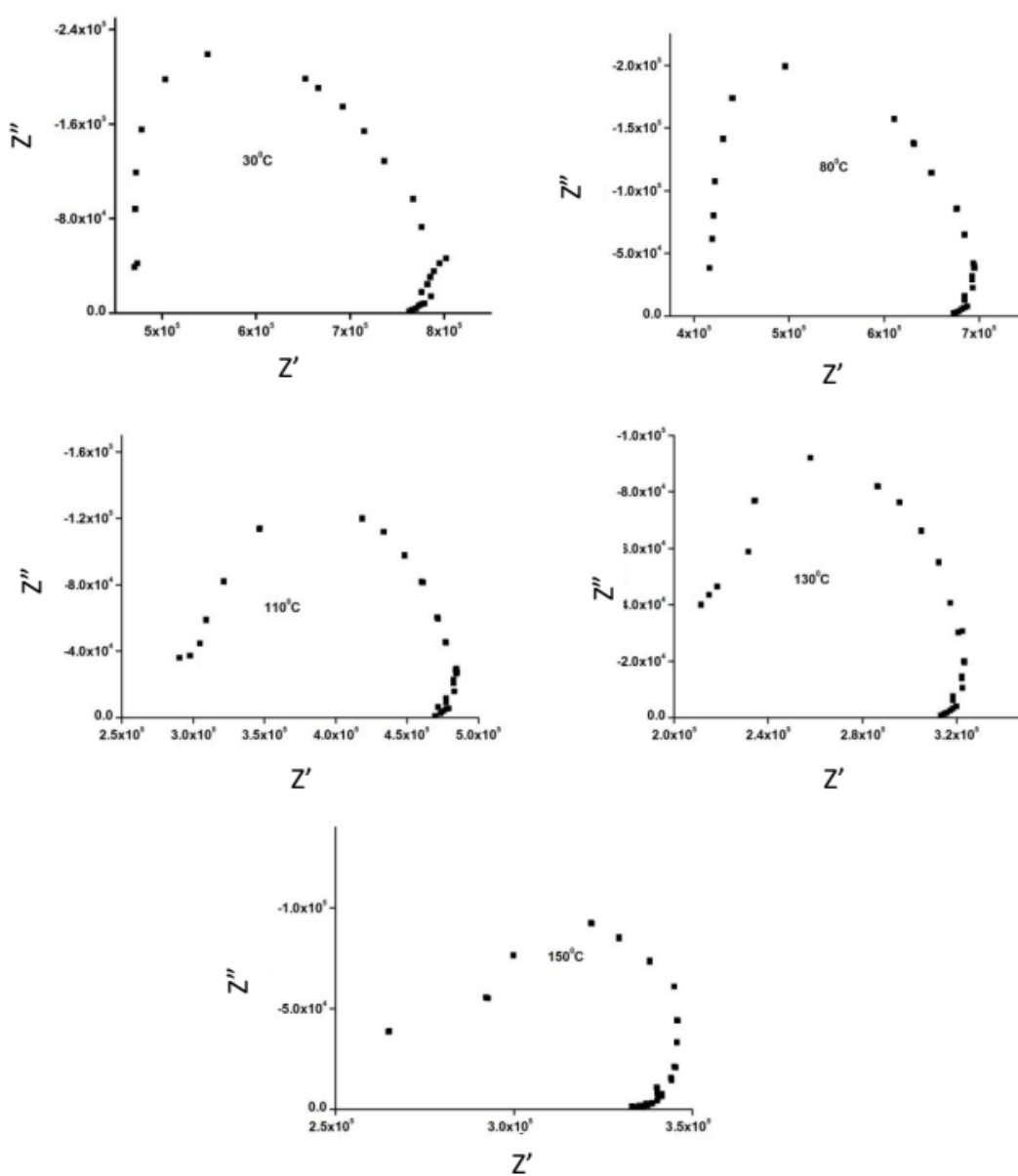


Fig 7.1 Impedance spectra of polypyrrole at various temperatures

Table 4.1 Impedance parameters for polypyrrole

S. No	Temperature In K	Bulk Resistance R_b (K Ω)	Bulk Capacitance C_b (10^{-12} F)	Relaxation frequency (Hz)	Conductivity $\times 10^{-9}$ (ohm-cm) $^{-1}$
1	303	325	0.2449	20000	2.04
2	353	277	0.2876	20000	2.41
3	383	193	0.8261	10000	3.46
4	403	115	153.71	9000	5.80
5	423	101	157.78	10000	6.61

The impedance spectra of copper ferrite at various temperatures are shown in Fig 7.2. The Nyquist diagram at room temperature is found to be very much distorted. At the intermediate temperatures 353 K and 383 K it can be seen that there are two effects pertaining to microstructural inhomogeneity - grain and grain boundary. Impedance spectroscopy allows the separation of the resistance related to grains and grain boundaries because

each of them has different relaxation times resulting in separate semicircles. The spectrum reveals a relatively large grain contribution to the total resistivity. The spectrum at 423 K has a perfect semicircle. The impedance parameters are found as said above and are tabulated (Table 4.2). It is found from the table that the conductivity value decreases as temperature increases. This shows that the copper ferrite has metallic type behaviour.

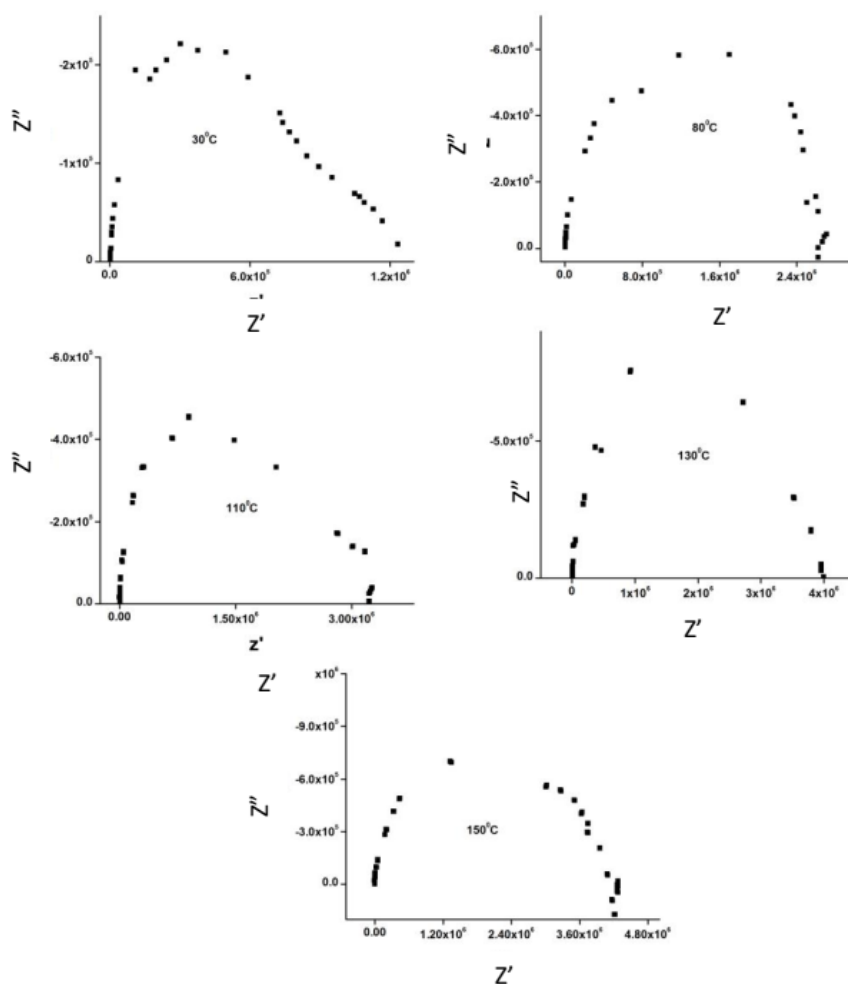


Fig 7.2 Impedance spectra of copper ferrite at various temperatures

Table 4.2 Impedance parameters for copper ferrite

S. No	Temperature (K)	Bulk Resistance R_b (K Ω)	Bulk Capacitance C_b (10^{-12} F)	Relaxation frequency (Hz)	Conductivity $\times 10^{-9}$ (ohm-cm) $^{-1}$
1	303	1257	211.08	600	1.91
2	353	2641	200.98	300	0.91
3	383	3110	170.69	300	0.77
4	403	3709	95.40	450	0.65
5	423	4280	186.018	200	0.56

The impedance spectra of CS I at various temperatures are shown in Fig 7.3. It is found from the spectrum that the plot doesn't coincide with the real axis. We are in need of high frequency measurements above 100 KHz to get a perfect semicircle. The peak gets broadened as the temperature increases indicating the multiple relaxations in the sample. The observation of single arc indicates that the circuit components of grain are much higher than that those of a grain boundary as the maximum of the arc in the

impedance plot shifts towards low frequency as the temperature increases. Additionally in the case of 303 K and 383 K are needs of data corresponding to frequencies below 1 Hz and above 100 KHz to get a perfect semicircle. The impedance parameters are found and are tabulated (Table 4.3). It is found that the conductivity of the sample increases as the temperature increases which shows that CS I has a semiconducting behaviour.

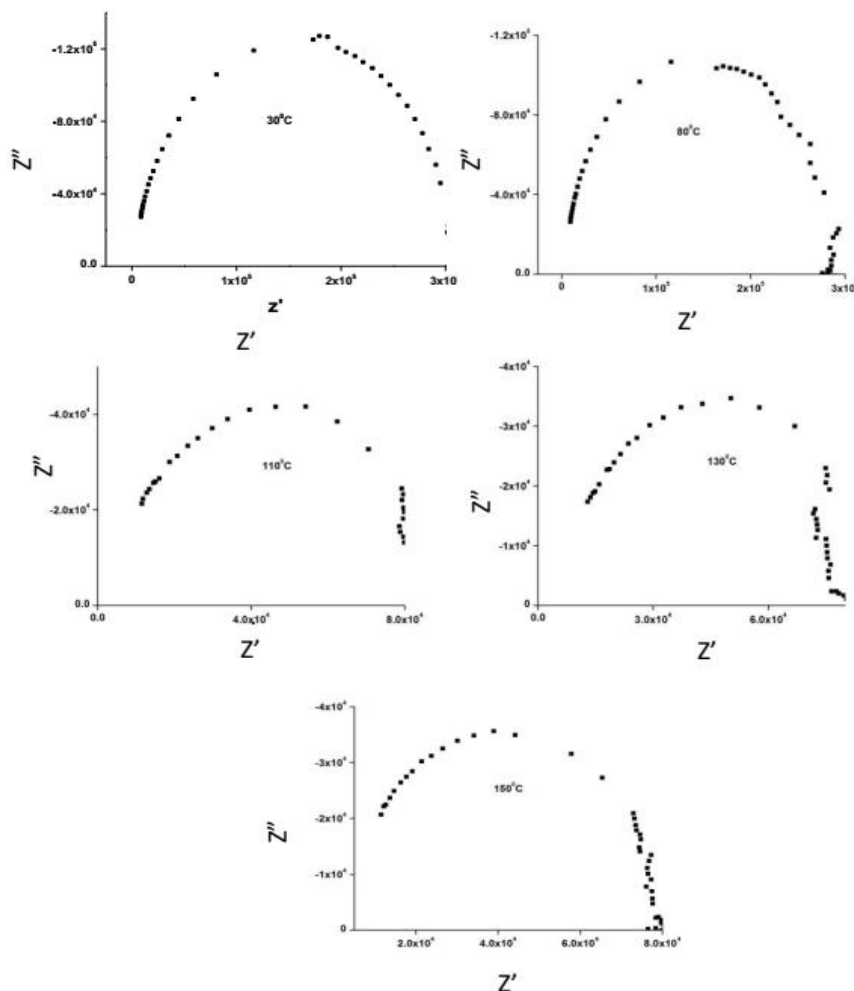


Fig 7.3 Impedance spectra of CS I at various temperatures

Table 4.3 Impedance parameters for CS I

S. No	Temperature (K)	Bulk Resistance R_b (K Ω)	Bulk Capacitance C_b (10^{-12} F)	Relaxation frequency (Hz)	Conductivity $\times 10^{-9}$ (ohm-cm) $^{-1}$
1	303	303	55.36	9500	1.07
2	353	278	38.24	15000	1.17
3	383	790	67.15	30000	4.10
4	403	733	72.40	30000	4.42
5	423	691	65.82	35000	4.69

The impedance spectra for the sample CS II at various temperatures are shown in Fig 7.4. It is found from the spectrum that at low temperatures there is a presence of a singular arc which suggests the presence of grain interior (bulk) property of the material. However, at higher temperatures another arc appears which shows that the

contribution to conductivity comes from both grains and grain boundaries. The impedance parameters are found and are tabulated (Table 4.4). It is found that the conductivity of the sample increases as the temperature increases which shows that CS II has a semiconducting behaviour.

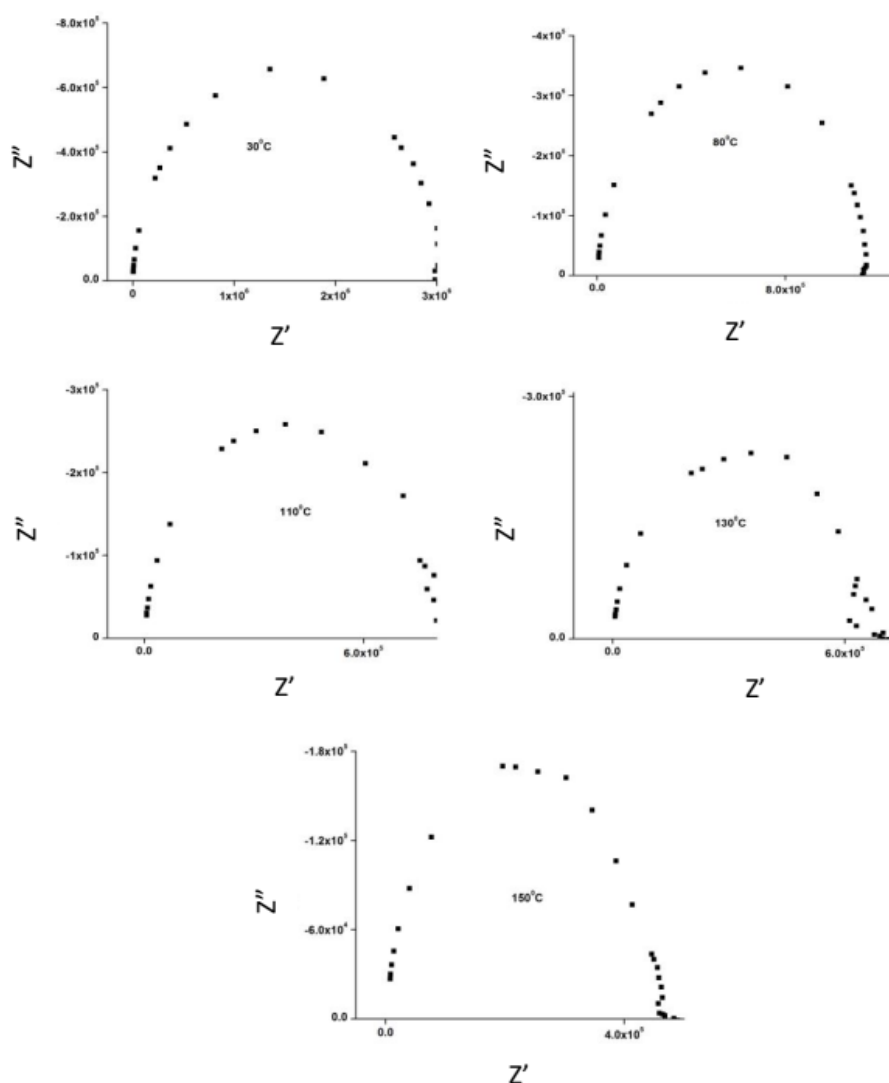


Fig 7.4 Impedance spectra of CS II at various temperatures

Table 4.4 Impedance parameters for CS II

S.No	Temperature (K)	Bulk Resistance R_b (K Ω)	Bulk Capacitance C_b (10^{-12} F)	Relaxation frequency (Hz)	Conductivity $\times 10^{-9}$ (ohm-cm) $^{-1}$
1	303	2968	17.88	3000	0.23
2	353	1136	31.15	4500	0.59
3	383	9512	27.90	6000	0.71
4	403	7024	37.79	6000	0.96
5	423	4603	34.59	10000	1.43

The impedance spectra for the sample CS III at various temperatures are shown in Fig 7.5. It is found from the spectrum that at all the temperatures there is a presence of a singular arc which suggests the presence of grain interior (bulk) property of the material. It is found that the plot doesn't coincide with the real axis. We are in need of high frequency measurements as in the case of CS I to get a

perfect semicircle. The impedance parameters are found and are tabulated (Table 4.5). It is found that the conductivity of the sample increases as the temperature increases which shows that CS III has a semiconducting behaviour. The Arrhenius plot of the all the samples are shown in Fig 8.

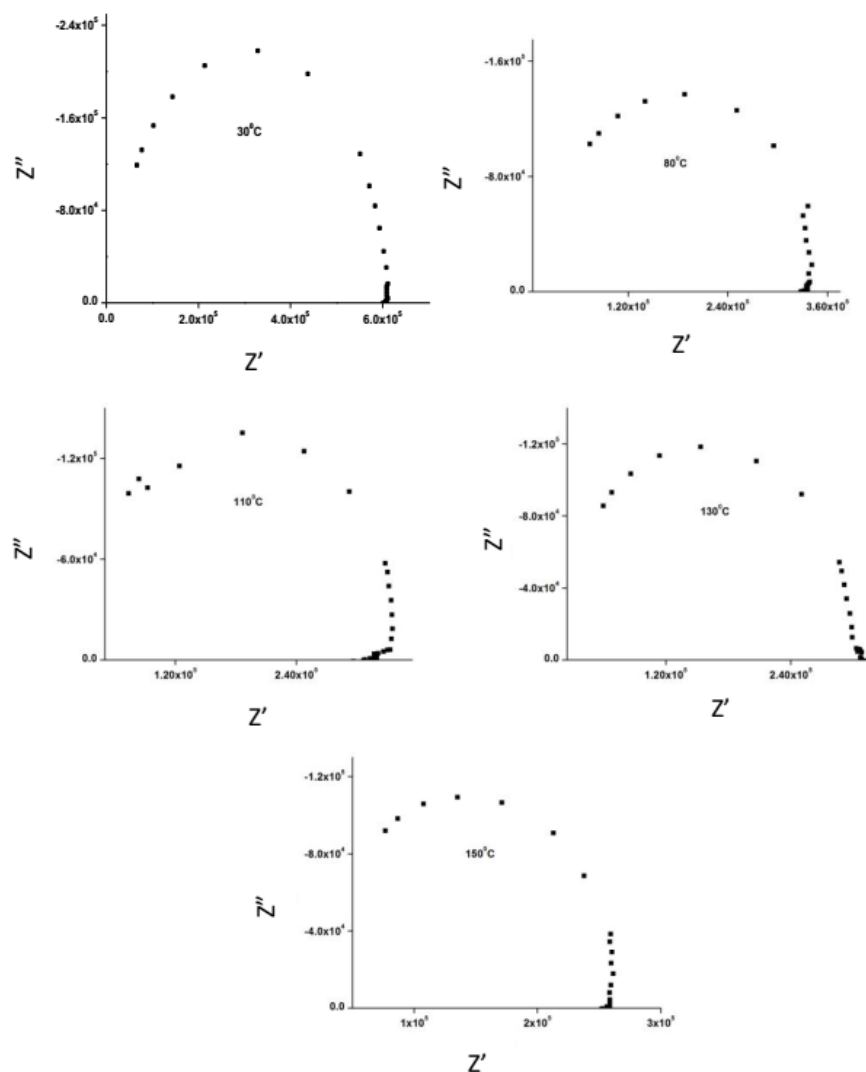


Fig 7.5 Impedance spectra of CS III at various temperatures

Table 4.5 Impedance parameters for CS III

S. No	Temperature (K)	Bulk Resistance R_b (K Ω)	Bulk Capacitance C_b (10^{-12} F)	Relaxation frequency (Hz)	Conductivity $\times 10^{-9}$ (ohm-cm) $^{-1}$
1	303	570	9.30	30000	1.06
2	353	278	12.74	45000	2.17
3	383	247	13.69	45000	2.33
4	403	246	14.34	45000	2.44
5	423	196	13.54	60000	3.08

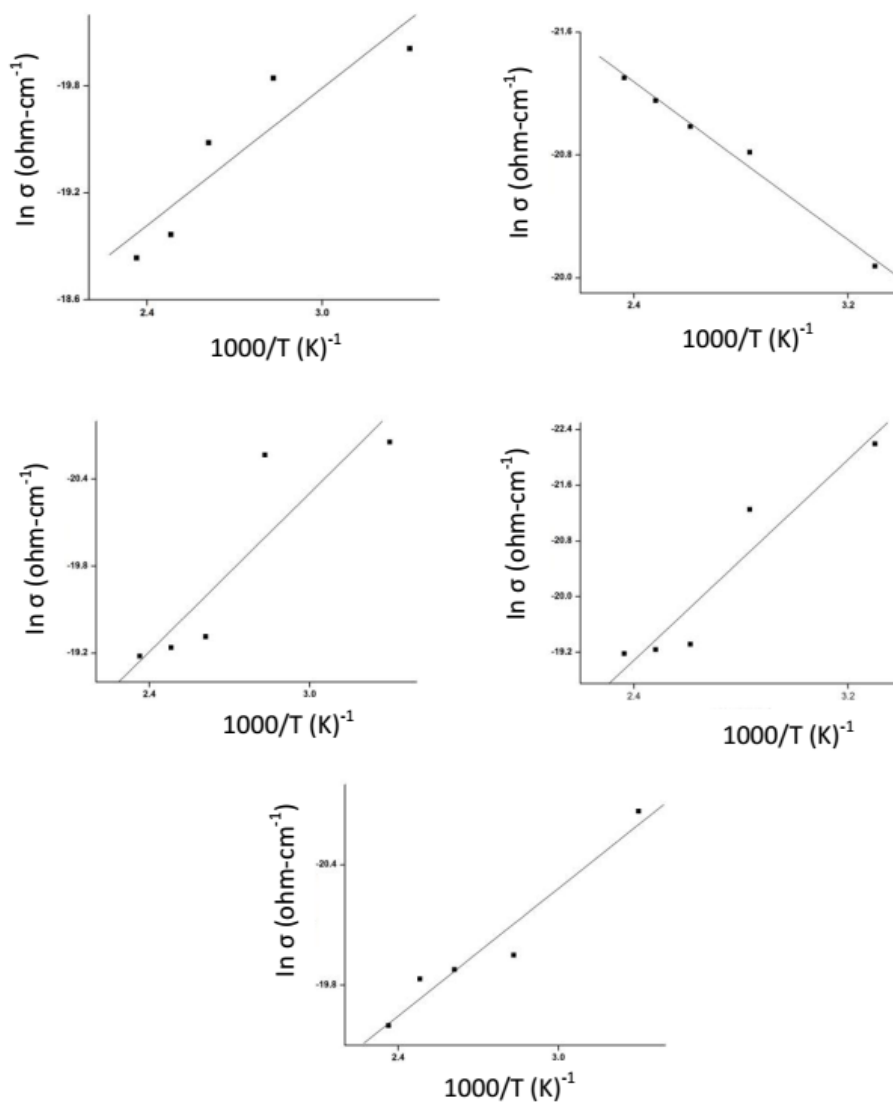


Fig 8. Arrhenius plot of PPy (8.1), CuFe_2O_4 (8.2), CS I (8.3), CS II (8.4), CS III (8.5)

4 Conclusions

Polypyrrole-copper ferrite nanocomposite is prepared with three different concentrations by in situ polymerization of pyrrole in aqueous solution. SEM studies reveal that the polypyrrole has a quasi-spherical structure. Copper ferrite sample has very fine particle size and hard nature. By polymerization of pyrrole monomers in the presence of copper ferrite, it is interestingly found that the produced composites possess sphere-like structure and no structure corresponding to copper ferrite powder was distinguished, which indicates that the copper ferrite is uniformly coated with polypyrrole and thus core-shell structure formed is confirmed in all the three composite samples. XRD studies results also show that there is no obvious chemical interaction between copper ferrite core

and polypyrrole shell. The grain sizes of the samples are found out using Debye-Scherrer formula. The strain in the prepared samples is found out using Williamson-Hall plot. Fourier Transform Infra Red spectroscopy studies results confirm the formation of polypyrrole and copper ferrite by the appearance of characteristic peak of polypyrrole and copper ferrite in the spectrum. All the composite samples are also found to have the characteristic peaks without any shift in the peak position and thus formation of core-shell structure is confirmed. Ultra violet spectroscopy studies show that the optical band gap of the material changes on addition of copper ferrite. The composite sample CS I is found to have higher optical band gap energy when compared to other two composite samples. A.C. conductivity studies give the electrical properties of the

prepared samples. Using A.C. impedance spectra, conductivities of all the five samples are found at various temperatures. The conductivity of the samples is found out using Nyquist diagram. In the case of CS I and CS III we are in need of high frequency measurements to get a perfect Nyquist diagram. The sample CS I is found to have high conductivity when compared to other two composite samples. Copper ferrite is found to have metallic type behaviour, while all other samples prepared are found to have semiconducting behaviour.

References

- [1] M. Y. Lo, C. Zhen, M. Lauters, G. E. Jabbour, A. Sellinger, *J. Am. Chem. Soc.* 129, (2007)5808.
- [2] P. G. Rickert, M.R. Antonio, M.A. Firestone, K.A. Kubato, T. Szreder, J. F. Wishart, M.L. Dietz, *J. Phys. Chem. B* 111, (2007) 4685.
- [3] P. Gomez-Romero, *Adv. Mater.*13, (2001)163.
- [4] S. C. Wuang, K. G. Neoh, E.T. Kang, D.W. Pack, D.E. Leckband, *J. Mater. Chem.* 17, (2007)3354.
- [5] X. L. Dong, X. F. Zhang, H. Huang, F. Zuo, *Appl. Phys. Lett.* 92, (2008)0143127.
- [6] S. M. Abbas, A.K. Dixit, R. Chatterjee, T. C. Goel, *Mater. Sci. Eng., B* 123, (2005) 167.
- [7] S. T. Selvan, J. P. Spatz, H. Klok, M. Moller, *Adv. Mater.* 10, (1998) 132.
- [8] S. Tian, J. Liu, T. Zhu, W. Knoll, *Chem. Mater.* 16, (2004)4103.
- [9] N. Murillo, E. Ochoteco, V. Alenanco, J. A. Pomposo, *Nanotechnology* 15, (2004) S322.
- [10] P. Xu, X. Han, C. Wang, H. Zhao, X. Wang, B. Zhang, *J. Phys. Chem. B* 112, (2008) 2775.
- [11] W. Zhong, S. Liu, X. Chen, Y. Wang, W. Yang, *Macromolecules* 39, (2006) 3224.
- [12] Ping Xu, Xijiang Han, Chao Wang, Donghua Zhou, *J. Phys. Chem. B* 112, (2008) 10443.